REPORT DOCUMENTATION PAGE

Form Approved OMB NO. 0704-0188

1. REPORT DATE (DD-MM-YYYY)	2. REPORT TYPE	3. DATES COVERED (From - To)
23-07-2009	Final Report	15-Sep-2008 - 14-Jun-2009

4. TITLE AND SUBTITLE
Surface Instabilities From Buried Explosives

5a. CONTRACT NUMBER
W911NF-08-1-0397

5b. GRANT NUMBER

5c. PROGRAM ELEMENT NUMBER
611102

6. AUTHORS
Leslie C. Taylor, William L.Fourney, Daniel P.Lathrop

5d. PROJECT NUMBER

5e. TASK NUMBER

5f. WORK UNIT NUMBER

7. PERFORMING ORGANIZATION NAMES AND ADDRESSES
University of Maryland - College Park
Office of Research Administration & Advancement
University of Maryland, College Park
College Park, MD 20742 -5141

8. PERFORMING ORGANIZATION REPORT NUMBER

9. SPONSORING/MONITORING AGENCY NAME(S) AND ADDRESS(ES)
U.S. Army Research Office
P.O. Box 12211
Research Triangle Park, NC 27709-2211

10. SPONSOR/MONITOR'S ACRONYM(S)
ARO

11. SPONSOR/MONITOR'S REPORT NUMBER(S)
54606-EG-II.1

12. DISTRIBUTION AVAILIBILITY STATEMENT
Approved for public release;distribution unlimited

13. SUPPLEMENTARY NOTES
The views, opinions and/or findings contained in this report are those of the author(s) and should not contrued as an official Department of the Army position, policy or decision, unless so designated by other documentation.

14. ABSTRACT
This report documents a preliminary study of surface instabilities that occur at the interface between soil and air during buried explosions. The purpose of understanding this instability is to determine its effect on local vehicle loading. Except when the target is on the surface, e.g., a tank track, the most important loading mechanism from a buried charge is the impact of soil propelled at the target by the expanding gas from the explosion. Detonation of a shallow buried explosive generally yields an unstable interface between the rising soil and the air. This unstable

15. SUBJECT TERMS
Buried Explosions, Richtmyer-Meshkov Instability, Target Loading, Jetting,

16. SECURITY CLASSIFICATION OF:			17. LIMITATION OF ABSTRACT	15. NUMBER OF PAGES	19a. NAME OF RESPONSIBLE PERSON
a. REPORT	b. ABSTRACT	c. THIS PAGE			William Fourney
U	U	U	SAR		19b. TELEPHONE NUMBER
					301-405-1129

SURFACE INSTABILITIES FROM BURIED EXPLOSIONS

Research Area 10
ARO Special Programs
Short Term Innovative Research (STIR) Program

Final Report
Grant No. W911NF0810397

21 July 2009

University of Maryland
College Park, MD

Leslie C. Taylor
William L. Fourney
Department of Mechanical Engineering and
Department of Aerospace Engineering
Daniel P. Lathrop
Department of Physics and
Institute for Research in Electronics and Applied Physics

Abstract

This report documents a preliminary study of surface instabilities that occur at the interface between soil and air during buried explosions. The purpose of understanding this instability is to determine its effect on local vehicle loading. Except when the target is on the surface, e.g. a tank track, the most important loading mechanism from a buried charge is the impact of soil propelled at the target by the expanding gas from the explosion. Detonation of a shallow buried explosive generally yields an unstable interface between the rising soil and the air. This unstable air – soil interface appears to be the result of Richtmyer-Meshkov instability. Irregular "fingers" of saturated sand extend into the air above a more generalized dome of soil. These fingers move at a much higher velocity than the material between them – especially at smaller stand off distances. As a result, the local load on the target at different positions on the target at the same distance from the charge may vary by 50% or more from shot to shot or even within a single shot . The variable nature of localized loading on the target requires a large design safety factor to assure vehicle integrity. This has important implications for efficient mine-resistant vehicle design.

Introduction

This report documents the results of a preliminary study of the surface instabilities that occur at the interface between soil and air during buried explosive detonations, in order to determine their effect on local vehicle loading. Except when the target is on the surface of the soil, e.g. a tank track, the most important loading mechanism from a buried charge is the impact of the soil propelled at the target by the expanding gas from the explosion. Efficient design to mitigate the damage to vehicles caused by detonations of buried explosives requires a detailed understanding of the loading.

The detonation of a buried explosive generally yields an unstable interface between the soil and the air as shown in Figure 1. Here, irregular "fingers" of saturated sand extending into the air above a more generalized dome are visible. The fingers are moving at a much higher velocity than the material between them. The existence of an irregular soil interface between the soil and the air when the burial depth of the charge is relatively shallow is more than just a detail; it affects the local loading (pressure) on the target vehicle. Figure 2 shows the local peak pressure as a function of horizontal distance from the center of the charge for a fixed height of target above the soil in three different nominally identical tests. The peak loads vary significantly from shot to shot. Figure 3 shows the results of two tests with rings of gages centered on the charge imposed on the same data as in Figure 2 [1]. This shows that even though the total force and total impulse transferred from an explosion to a target are fairly repeatable, the pressures, i.e., the local load on the target, at different positions on the target surface at the same distance from the charge may vary by 50% or more in a single shot. This has important implications for efficient mine-resistant vehicle design; the variable nature of local surface pressure on the target requires a large design safety factor to assure vehicle integrity.

The unstable air – soil interface appears to be a product of Richtmyer-Meshkov instability (RMI). RMI occurs when an incident shock accelerates an interface between two fluids of different densities and thus amplifies any initial perturbation present on the interface.[2] Saturated sand and air differ in density by a factor of about 1500, so this effect is quite pronounced in the cases of interest here. (In most instances of RMI studied in the past, the densities of the two fluids differed by a factor of about 6 or less [2].) RMI is initiated by an impulsive load, such as a significant pressure pulse or shockwave, when the pressure and density gradients are misaligned at the interface. Preliminary tests with prepared depressions in the soil suggested that the "misalignment" of the soil – air interface is the product of pre-existing, random, depressions in the soil surface. In the case where a heavy fluid penetrates a light fluid, RMI typically features spikes of the heavy fluid penetrating the light one, as is shown in Figure 1. Since the distribution of sizes and locations of irregularities in the soil surface is random and presumed to be chaotic, certainly the distribution of the locations of the pressure spikes will then be chaotic and most likely their velocities will be as well.

In this preliminary study, we have focused on the effect of depressions in the soil surface in creating jets (fingers) and on determining the velocity of the jets, rather than on the

chaotic nature of the soil surface in the real world. Preliminary tests showed that the deeper the charge is buried, the smoother the interface between the soil and the air. Compare Figure 4, where the charge was quite deep with Figure 1. At this time we believe the interface between the soil and the air is smoother for deeply buried charges because the pressure pulse initiating the jets has a lower peak pressure and longer rise time. This belief should be investigated in more detail in future studies. In the tests reported herein, the charge was quite deeply buried so that the effect of the natural depressions in the soil surface did not overwhelm the effect of the planned depressions.

To provide insight into the results to be expected from our test program, as a favor, Dr. Andrew Wardlaw provided a computation for a case where the charge is relatively deeply buried below a conical indentation in the surface of the soil [3]. The geometry of the computation was actually that of the Dome 29 test, Table 1. This clearly showed that jetting is dominantly a shockwave – driven process and that the rising of the dome of soil is driven primarily by the expanding gas bubble. Figure 5 shows the computed density of the sand at various times. Notice in Figure 6, a detail of Figure 5d, that while the material under the surface of the dome cavitates and the density of the soil in this region can be, briefly, fairly low, the density of the jet is about 90% of that of the pretest soil. This is consistent with the view suggested by Figure 2 that the impact (stagnation) pressure caused by a jet can be quite high.

The variables most significant in the formation of jets or fingers of soil appear to be the charge size (W), the depth of burial (DoB) of the charge and the size of the depression in the soil. Thus, the test program was structured to systematically explore the effect of varying these parameters. In the tests conducted in this program, all of the soil depressions were made with cones with a 45° half-angle, so size of the depression can be characterized by the diameter of the cone used to make the depression in the sand surface. Not only were the charge size, depth of burial and cone diameter systematically varied, some of the values of these variables were chosen to investigate the scalability of the jetting phenomenon.

Test Program

We conducted 16 tests, 14 of which produced data, as shown in Table 1. The soil in which the charge was buried was water – saturated sand. The grain size distribution in the two sand beds used is shown in Figure 7. Three charge sizes were used; 0.5 g, 4.0 g and 0.069 g. The "standard" charge size was 0.5 g, which we have used in previous tests to observe the interface between the rising soil and the air. When this is scaled up by a factor of 2, using $W^{1/3}$ scaling, the result is 4.0 g. The 0.5 g and 4.0 g charges were made up of DETASHEET explosive containing 63% PETN and an RISI RP-87 detonator. The charge weight given here is the weight of the PETN in the DETASHEET plus the RDX and PETN in the RP-87. Figure 8 shows a typical charge. When the 0.5 g charge is scaled down by a factor of 2, a charge weighing 0.0625 g results. However, the smallest charge we can easily work with is a single RP-87 detonator containing 0.069 g of RDX and PETN. This is a 10% mass error, larger than might be desired, but since it is only a 3% scale error, we do not believe it has a significant effect on the results or conclusions.

All of the data were gathered visually using high speed video. We used a Phantom v120 video camera and most of the data were taken at 180,000 frames per sec (5.5 μs per frame), with some of the 4.0 g tests videoed at 140,000 frames per sec. The position of the resulting jet and dome of sand were digitized, frame by frame, and put into Excel spreadsheets for analysis. The tests with the 0.5 g and 0.069 g charges were conducted in a test bed that is 3in. wide by 35 in. long with transparent sides so the event could easily be viewed using a high speed video camera essentially level with the level of the sand. See Figure 9. In order to avoid destroying this test bed, the tests with 4.0 g charges were carried out in our 5 ft by 5 ft sand test bed.

In each of the tests, a small cone, with a 45° half-angle, Figure 10, was pressed into the sand surface to create a controlled depression in the soil directly above the centerline of the charge. (In test "Dome 43" a second, off-center depression was also present.) Three cone sizes were used: 0.5, 0.25 and 0.125 in. in diameter. Some tests were repeated, either to get some insight into repeatability or to make up for poor data. In test Dome 38, not listed in Table 1, the camera failed to trigger and no data were gathered.

The variables considered in this test program were the charge size (W), the depth of burial (DoB) of the charge and the diameter of the cone used to make the depression in the sand surface. The tests can be divided in four groups. Test Dome 30 can be thought of as the 'central' test and all the others as variations of it. Table 2 shows the tests used to investigate the scalability of the jetting phenomenon. In the tests shown in Tables 3, 4 and 5 each of the three parameters was varied, with the other two held constant.

Table 1 shows the test conditions for the Dome 30 test. Figure 11 shows the surface of the sand prior to the test. The cone diameter is 0.25 in. To provide a scaled distance to enable data reduction, the two pieces of black tape are two inches apart. The next two figures come from the high speed video of the event. Figure 12a shows the jet just beginning to form and Figure 12b shows the jet fully formed. Notice the spray from the surface of the sand. This spray often made it difficult to determine the exact location of the top of the dome of sand developed by the explosive. This figure also shows smaller jets forming farther from the center of the charge, based on natural depressions between the larger grains of sand.

Test Results and Discussion

The test results seem to be reasonably repeatable. The test conditions of Dome 30, Dome 43 and Dome 44 were nominally identical. Figure 13 shows the location of the jet tip as a function of time in each of these cases. Figure 14 shows the location of the top of the dome in these tests. The dispersion is greater in the latter case, but the top of the dome is more difficult to track than the jet because of the spray over the top of the dome. In both cases, the line labeled "Target" is where a target 16 in. above the ground would be if the charge weighed 10 lb. This is the case in all figures where there is a line labeled "Target."

Figure 15 shows all of the jetting data believed to be valid from the tests of Table 2, which includes only tests that are scaled versions of each other. The time and position have been brought to a common scale by dividing them by $W^{1/3}$. It suggests that the jetting, or finger, process scales reasonably well, at least over the range of values used in this test program. The linear scale factor from the largest to the smallest charge is four. Given the difficulty in placing the charge accurately in depth and the difficulty in digitizing the high speed video, the dispersion at a height equivalent to 16 in. for a 10 lb charge is remarkably small. Figure 16 shows the location of the top of the soil domes as a function of time. Again the data have been reduced by the factor $W^{1/3}$, to bring them to a common scale. In this case, the dispersion is larger than in the case of the jets, but because of the initial spray caused by the shockwave's reflecting from the surface, the actual surface of the dome is more difficult to discern and hence, harder to digitize accurately.

Notice, in Figure 15, the curves are generally concave downward: The jets are slowing with time. However, the curves in Figure 16 are generally concave upward: The domes are still accelerating. Jetting is driven by the shock output of the charge. The jet acquires its maximum speed very quickly, even on the time scales used in these tests, and then starts losing velocity almost immediately. Rising of the dome, on the other hand, is driven by the expanding gas bubble and takes place over a time period comparable to the one in these experiments. This suggests that if the target is far enough away, the jetting, or finger, effects are of reduced importance. This emphasizes that in considering the buried IED problem, near-field effects are unusually important.

Figure 17 shows the position of the domes and the jets for three different sizes of cones. It is not necessary to use reduced values to compare these results since all of the tests were conducted with the same size charge and the same DoB. The positions of the three domes as a function of time are essentially the same, as they should be, since all of the tests were conducted with the same charge size and DoB. At the scale we are interested in in this investigation, i.e., quite small depressions in the soil surface, the size of the depression has no effect on the height of the dome as a function of time. However, if we consider the position of the jet relative to the to surface of the dome, rather than its absolute position, Figure 18, the jets from the 0.125 in. and 0.25 in. cones have about the same position as a function of time, whereas the jet from the 0.5 in. cone has a somewhat higher velocity. This is very little data on which to base a conclusion, but the data do suggest that there may be some depression size, below which the jetting phenomenon changes little with the size of the depression in the soil.

When the DoB is varied, with the charge mass and the size of the depression in the soil held constant, as shown in Table 4, it appears that, over the time interval examined in these tests, the peak (i.e., initial) velocity of the jet decreases at somewhat less than the -2 power of the reduced DoB. Figure 19 shows the position of the jets as a function of time. Figure 20 shows the initial velocity of the jet as a function of reduced DoB. This curve was developed by fitting a curve to the data of Figure 19 and differentiating the equation of the curve with respect to time and then finding the velocity when the height of the jet is zero. It shows that the initial velocity of the jet falls off with increasing reduced DoB

at somewhat less than the -2 power. The initial velocity of the dome raised by the gas bubble can be viewed the same way. It decreases much more rapidly with increasing reduced DoB than does the initial velocity of the jet. Note, however, in Figure 21, that in any one event, the velocity of the dome increases with time. The initial velocity of the dome is not its peak velocity. This is a bit hard to see in the case of the Dome 35 dome in which the DoB of the charge was only 0.595 in. However, a careful examination of this curve show that the velocity of the dome does, in fact, initially increase after forming, though it eventually starts to decrease. Because of its shallow burial and the consequent reduced mass of soil over the charge, it accelerates very much more rapidly than the others, reaches a peak velocity very quickly and then starts to decrease.

The set of tests in which the size of the charge was varied with the DoB and size of the depression in the soil held constant, shown in Table 5, can be related to the previous set of tests. Figure 22 shows the reduced position of the jets and domes as a function of reduced time. Not surprisingly, the larger the charge, all else the same, the faster the jets and domes rise. However, if curves are fitted to these data and differentiated in the same way as in the set above, in which the DoB was varied, we can determine the initial velocity of these jets as a function of reduced DoB. When these data are plotted on the same graph with the jet data above, Figure 23, we obtain a line with a different slope. In this case, the velocity of the jet decreases with increasing reduced DoB at more than the -2 power. At this time we have no explanation for this difference. There are several possible reasons for this discrepancy, not the least of which is that the data set is very small and this merely represents scatter in the data. However, the difference is large enough that we feel that the difference could be real. It could be that the scaling method used here (developing reduced values of the data with the factor $W^{1/3}$ power) is inadequate. In any case this issue merits further investigation.

In addition to the tests described above, several addditional tests were conducted to explore other aspects of the jetting (finger) phenomenon. These are described below.

One of the mechanisms postulated for the development of fingers or jets when a charge is detonated with a soil overburden, especially a sandy soil, is the existence of “chains” of grains of sand that can transmit forces, more directly and with less damping than can the bulk of the soil [4]. We conducted two tests in which we embedded pre-formed chains of sand grains in the soil above the charge. Both were conducted with 0.5 g charges. One was buried 1.19 in. deep; the other, 0.19 in. deep. The pre-formed chains were constructed by making a very small diameter hole in a piece of wax, filling the hole with sand and a very low viscosity epoxy. Once the epoxy was fully hardened, the wax was melted away leaving a thin, pre-formed chain of sand grains. These pre-formed chains were embedded in the sand above a buried charge in tests which were viewed using very high speed video (100,000 and 180,000 frames / sec). There did not seem to be any preferential location of the fingers or jets in the resulting soil movement. As a result, we have concluded that this is not a likely source of the fingers that are formed when a buried charge detonates.

In test Dome 43 there were two indentations in the soil, both made by the 0.25 in. diameter cones. One indentation was centered on the charge, as in test Dome 30. The other was centered three cone radii (0.375 in.) to one side. Since the charge is 0.250 in. in radius, this puts the offset cone near the edge of the charge in plan view. Figure 23 shows the positions of the two jets at two different times. The initial velocity of the center jet was 7190 in/sec. The initial velocity of the offset jet was 6287 in/sec. However, the DoB of the charge was 1.19 in., quite deep. Thus the shock wave was nearly spherical by the time it reached the conical indentations in the soil. See Figure 5. Therefore, it traveled slightly farther to the off-center charge. Even so, the difference in the velocities of the two jets is only a little more than the difference in vertical velocity between the two points on the dome of sand pushed up by the gas bubble.

In test Dome 44, we used black sand to investigate sand mixing in the jetting process. The charge size, DoB and cone size were the same as in test Dome 30. Figure 25 shows a pre-test view with the 0.25 in. cone still in place. It was removed before the test. The center circle of black sand is .05 in. in diameter. The outer black ring has a 1.0 in. inner diameter and a 1.5 in. outer diameter. The black sand was 0.5 in. deep, so it extended below the indentation made by the 0.25 in. cone. High speed videos of the test from above and from the side showed no apparent mixing of either the inner black circle of sand or the outer ring with the other sand over the time interval in which we are interested. See Figures 26 and 27.

Conclusions

A comparison of the three essentially identical tests, Domes 30, 43 and 44 shows that the results of this kind of testing are repeatable provided the initial conditions are the same. This shows that a further, more extensive experimental investigation of the jetting or finger phenomena is likely to be useful. The formation and evolution of the jets and domes seem to scale reasonably well. Figures 15 and 16 showed that, over the range of scale considered her, the position of the tip of the jet and the top of the dome appear to scale reasonably quite well. However, Figure 23 suggests that further investigation is needed to ensure that the scaling method used in this report, $W^{1/3}$, is fully adequate.

It does not appear that “force chains” of sand which can form and transmit loads through sand independently of the bulk of the material are a likely driver of the jets seen in uncontrolled buried explosions. Two tests with artificial chains of sand showed no preferential formation of jets. As a result of these two tests and the fourteen tests with depressions in the surface of the soil, we feel that the most likely source of the random or chaotic jetting encountered in uncontrolled buried explosions is the shockwave (or pressure pulse) from the detonation interacting with the random or chaotic natural depressions in the surface of the soil. This is consistent with the definition of RMI.

The shockwave or steep-fronted high pressure pulse drives the formation of the jets or fingers, which are characteristic of RMI. The motion of the bulk of the material directly above the charge, the dome, is driven by the expansion of the explosive gas bubble. These conclusions seem intuitively reasonable and are supported by the result of a limited

computational effort. The jet accelerates very rapidly, and then slows, presumably due to gravity and air drag, over the time period investigated in this effort. The dome generally accelerates continuously throughout the time period of interest in this investigation, that is, up to about one millisecond. This suggests that at some point, the difference between the dome and jet velocities will become unimportant. It emphasizes that in the case of buried mines and IEDs near-field effects are unusually important.

The DoB of the charge and the weight of the charge are related in the function (DoB/ $W^{1/3}$), the reduced DoB. The peak velocity of the jet, which is its initial velocity, decreases as the charge is either reduced in weight or buried deeper. The present data show that when the DoB is increased, the initial velocity of the jet decreases at slightly less than the -2 power of the reduced DoB, but when the charge weight is decreased, the initial velocity of the jet decreases at slightly greater than the -2 power of the reduced DoB. At this time it is unclear whether this is due to the scatter in the data which must be expected when one is dealing with soil as a medium or whether a different form of scaling might be needed. It should be noted that in most cases dealing with shock effects, $W^{1/3}$ scaling works quite well and the jetting process appears to be a shock driven process.

The sand in the jet can be thought to have "liquefied," somewhat after the fashion of the jet from a shaped charge warhead. However, there does not appear to be any other visual evidence of liquefaction of the sand – water mixture. The test with colored sand showed that there is very little mixing of the soil in the time period of interest to this problem. When all of the tests with depressions in the soil are viewed as a whole, it appears that depressions in the surface of the soil of the size tested in this program have little or no effect on the motion of the soil dome.

We conducted one test with two equal size depressions in the soil. One was centered over the charge. The other was near the edge of the charge, in plan view. The velocity of the off-center jet was 88% of that of the on-center jet, showing that the jet velocity does not fall off much with location of the depression, provided it is within the diameter of the charge, even when the charge is quite deep. This seems consistent with the high-speed video picture shown in Figure 1. Notice that, in this view, the size of the jets (fingers) falls off very quickly beyond the radius of the charge.

Recommendations

Because the interaction between the explosion of a buried charge and the target takes place in the near-field of the explosion and causes large variations in the local loading on the target, quantifying the finger or jetting phenomenon is important in designing vehicles better to resist buried mines and IEDs. Consequently the problems discussed in this report merit further exploration, both experimentally, and with support by computation using a good Eulerian code with a good soil model. Computational support of an experimental effort is very important. It provides insight into the processes involved that is sometimes very difficult to gain experimentally. Even the very limited

computational support we obtained for this effort was quite useful. Among other things, it showed that the density of the material in the jet is a quite high percentage of the pre-test density of the soil. This emphasized that the jets can contribute significantly to the load on the target.

One of the issues not dealt with in this preliminary study is the surface of the soil. There should be a study of the roughness of the soil and how the roughness is distributed not only spatially, but also in the frequency of sizes and shapes of indentations. There should be an attempt to characterize the roughness, perhaps statistically. In this program, we originally planned to conduct some explosive tests with saturated sand which has a much coarser grain size, but we ran out of time and money before we could conduct these tests. The coarser grain size would provide larger "natural" indentations in the surface.

Further investigation of this phenomenon should also include different geometries of depressions in the soil: different cone angles, as well as non- conical shapes such as those with rounded bottoms or pyramidal shapes. In the natural environment, the size and shape of the depressions in the surface of the soil is, in part, a function of the size and shape of the particles making up the surface of the soil, therefore they can have a variety of shapes and sizes. The tests in which the depression in the soil was varied while the charge size and DoB were held constant suggest that there may be a depression size below which the jet velocity changes little. This should also be investigated further.

Additional tests are needed in which the impact (stagnation) pressure of the jets and domes are measured while they are being recorded with high speed video. This will provide a correlation between the measured velocity of the jet and dome and the pressure on the target. This, of course, enables one to determine the effective density of the material actually hitting the target using Bernoulli's Law, and provide confirmation of the computational model being used.

The sand dome raised by the expanding explosive gas bubble is smoother when the charge is deeper. That is, jetting decreases and effectively disappears if the charge is deep enough. We believe this effect may be related to the peak pressure in the shockwave / pressure pulse that drives the jetting, or to its shape or to both. Further effort should include measuring the pressure in the soil as a function of time during the explosive event. This has been done successfully on a larger scale using tourmaline pressure gages, for example, [5]. With quite small tourmaline pressure gages, it should be possible to do so in small scale tests as well. Measuring the pressure will enable one to address the effect of changes in the shockwave as it progresses toward the surface of the soil on the intensity of jetting at the surface of the soil. This will also provide insight into the issues related to the discrepancy between the effect of DoB and charge weight shown in Figure 23.

Acknowledgements

This material is based upon work supported by the U. S. Army Research Office, Dr. Bruce LaMattina, under grant number W911NF0810397. The authors also wish to thank

the following people who made significant contributions to this effort. Dr. Andrew Wardlaw used his own time to provide hydrocode computations for us. The explosive tests were conducted in Dynamic Effects Laboratory of the University of Maryland largely by undergraduates, Dana Colegrove, Scott Yamada and Tom Brodrick, under the supervision of Ulrich Leiste.

References

1. Taylor, L.C., Fourney, W.L., Leiste, H.U., & Cheeseman, B., *Loading Mechanisms on a Target from Detonation of a Buried Charge*,. Proceedings of the 24th International Symposium on Ballistics, New Orleans, LA, 22 – 26 September 2008

2. Palekar, A., Vorobieff, P., Truman, C. R., *Two-dimensional Simulation of Richtmyer-Meshkov Instability*, submitted to Fluid Dynamics Researc*h*, Sept. 2004.

3. Wardlaw, A., Personal Communication, 17 Feb, 2009

4. Cates, M.E., Wittmer, ,J.P., Bouchaud, J.-P., & Claudin, P., *Jamming, Force Chains and Fragile Matter*, Physical Review Letters, Vol. 81, No. 9, p. 1841, August 1988

5. Taylor, L.C., Fourney, W.L., & Robeson, D.E., Spring 1998 Explosive Testing at Port Wakefield, Australia Including Explosive Cratering and Channeling, IHTR 2188, Incian Head Division, Naval Surface Warfare Center, July, 1999

Table 1 Tests and Test Conditions

Dome Number	Cone Dia [in.]	DoB [in.]	Charge Mass [g]	Comment
29	0.5	1.19	0.5	
30	0.25	1.19	0.5	
31	0.5	2.38	4	
32	0.125	0.595	0.069	
33	0.25	2.38	0.5	
35	0.25	0.595	0.5	
36	0.25	1.19	0.069	
37	0.125	1.19	0.5	#34 Replacement
39	0.25	1.19	4	Poor data
40	0.25	1.19	4	Re-run of #39
41	0.5	1.19	4	Re-run of #31
42	0.125	0.595	0.069	Re-run of #32
43	0.25	1.19	0.5	Variant of #30 Two cones
44	0.25	1.19	0.5	Variant of #30 Colored sand

Table 2 Scaled Tests

Test Number	Cone Dia [in.]	DoB [in.]	Charge Mass [g]
41	0.5	2.38	4
31	0.5	2.38	4
30	0.25	1.19	0.5
43	0.25	1.19	0.5
44	0.25	1.19	0.5
32	0.125	0.595	0.069
42	0.123	0.595	0.069

Table 3 Cone Size Varied, all else Constant

Test Number	Cone Dia [in.]	DoB [in.]	Charge Mass [g]
29	0.5	1.19	0.5
30	0.25	1.19	0.5
43	0.25	1.19	0.5
44	0.25	1.19	0.5
37	0.125	1.19	0.5

Table 4 DoB Varied, All Else Constant

Test Number	Cone Dia [in.]	DoB [in.]	Charge Mass[g]
33	0.25	2.38	0.5
30	0.25	1.19	0.5
43	0.25	1.19	0.5
44	0.25	1.19	0.5
35	0.25	0.595	0.5

Table 5 Charge Size Varied, All Else constant

Test Number	Cone Dia [in.]	DoB [in.]	Charge Mass [g]
40	0.25	1.19	4
30	0.25	1.19	0.5
43	0.25	1.19	0.5
44	0.25	1.19	0.5
36	0.25	1.19	0.069

Figure 1 Frame From High-Speed Video, 0.8g Charge, DoB = 0.39 in.

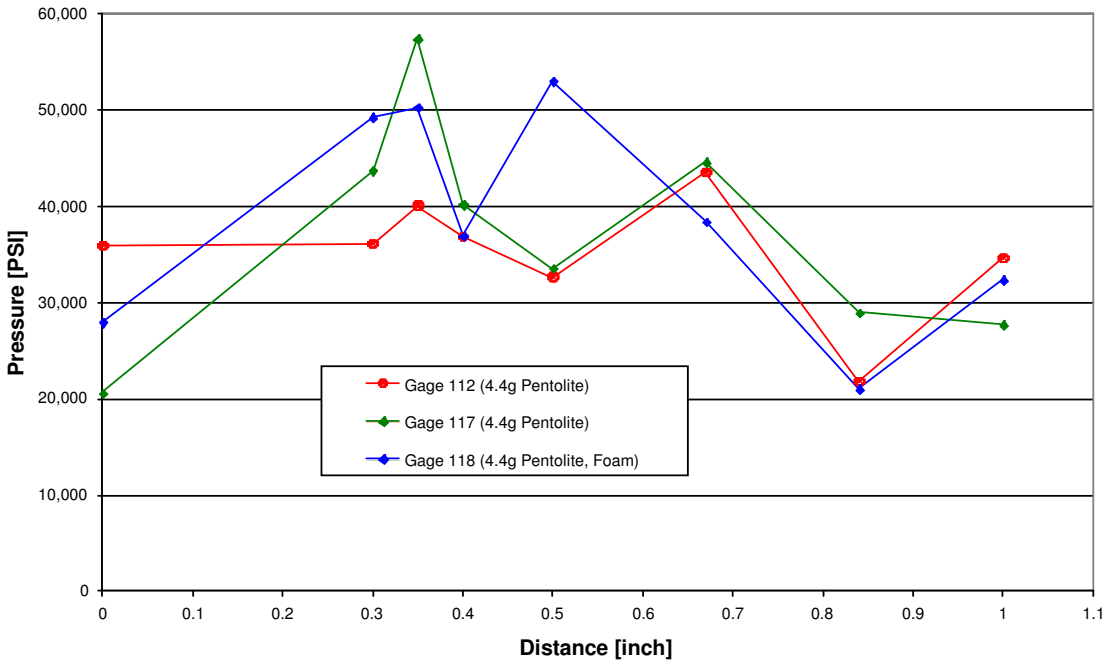

Figure 2 Peak Pressure vs Distance From Charge Centerline, Three Tests

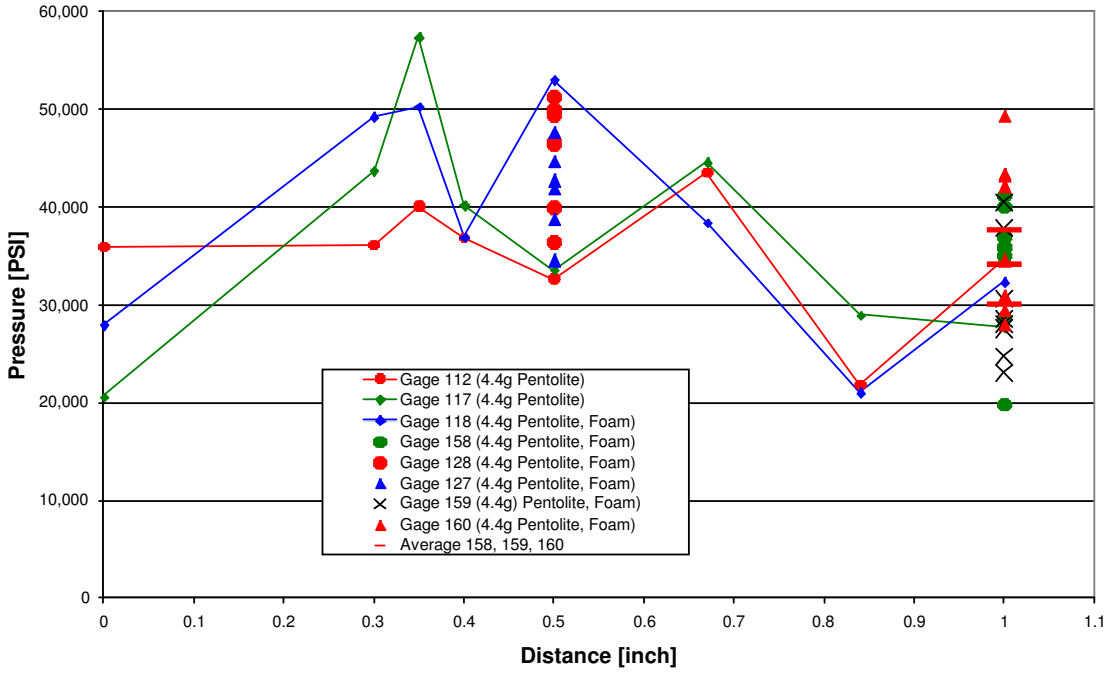

Figure 3 Peak Pressure vs Distance From Charge Centerline With Additional Data

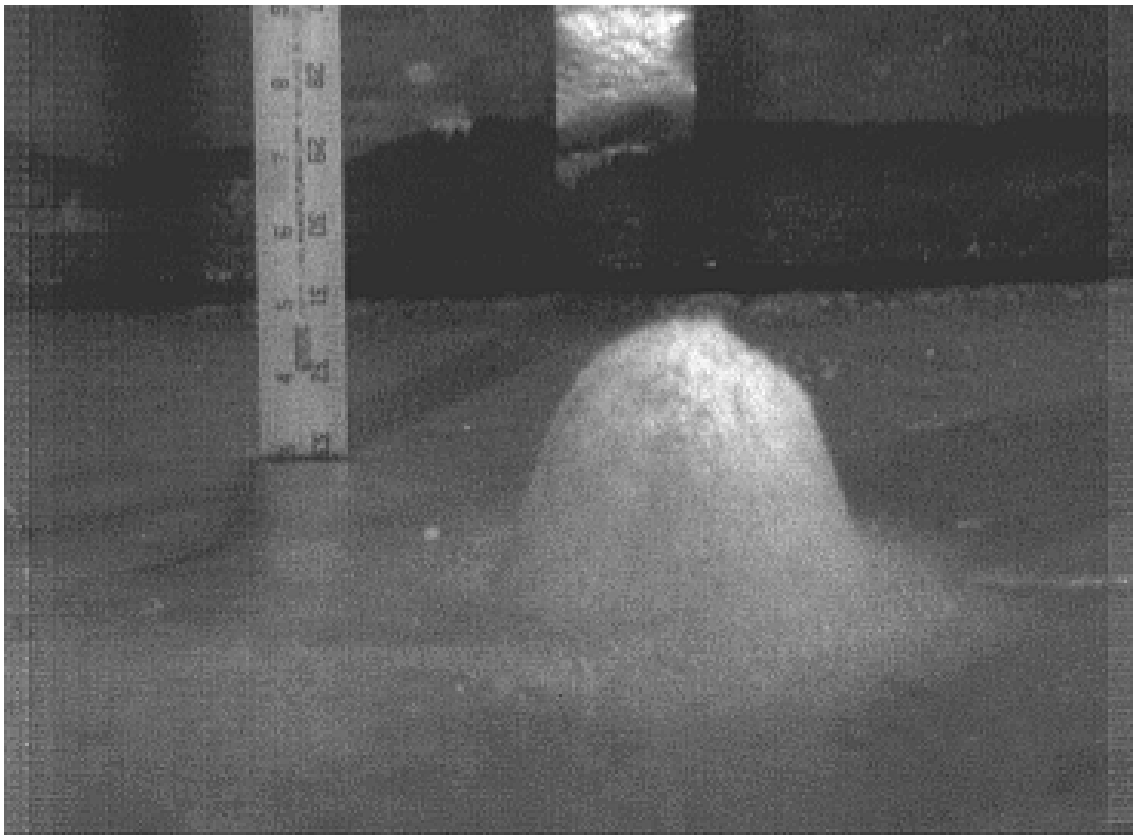

Figure 4 Frame From High-Speed Video, 0.5g DETASHEET Charge DoB = 1.19 in.

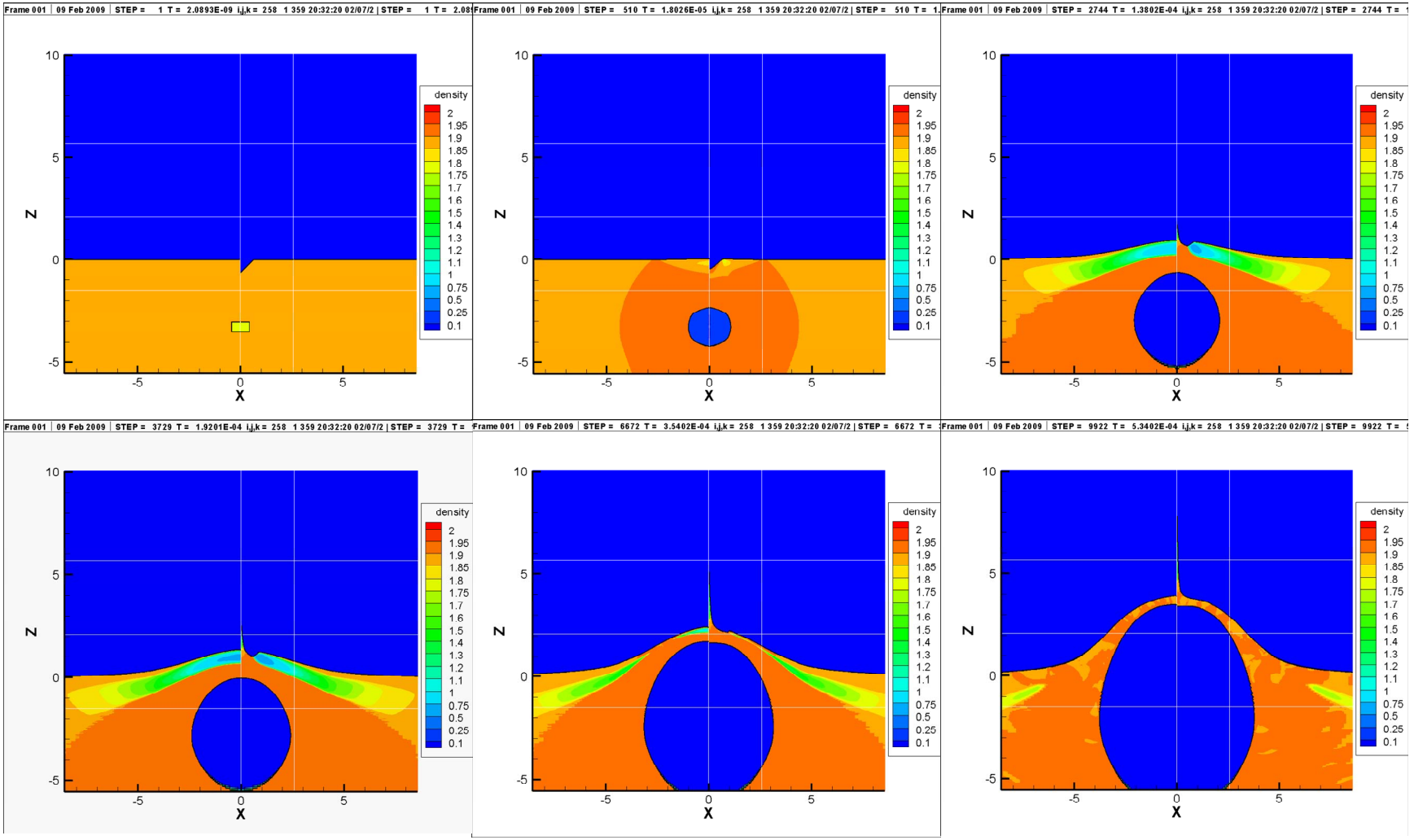

Figure 5 Computed Result, 0.5g DETASHEET Charge, DoB = 1.19 in., 0.5 in. Dia Cone on Right, No Cone on Left

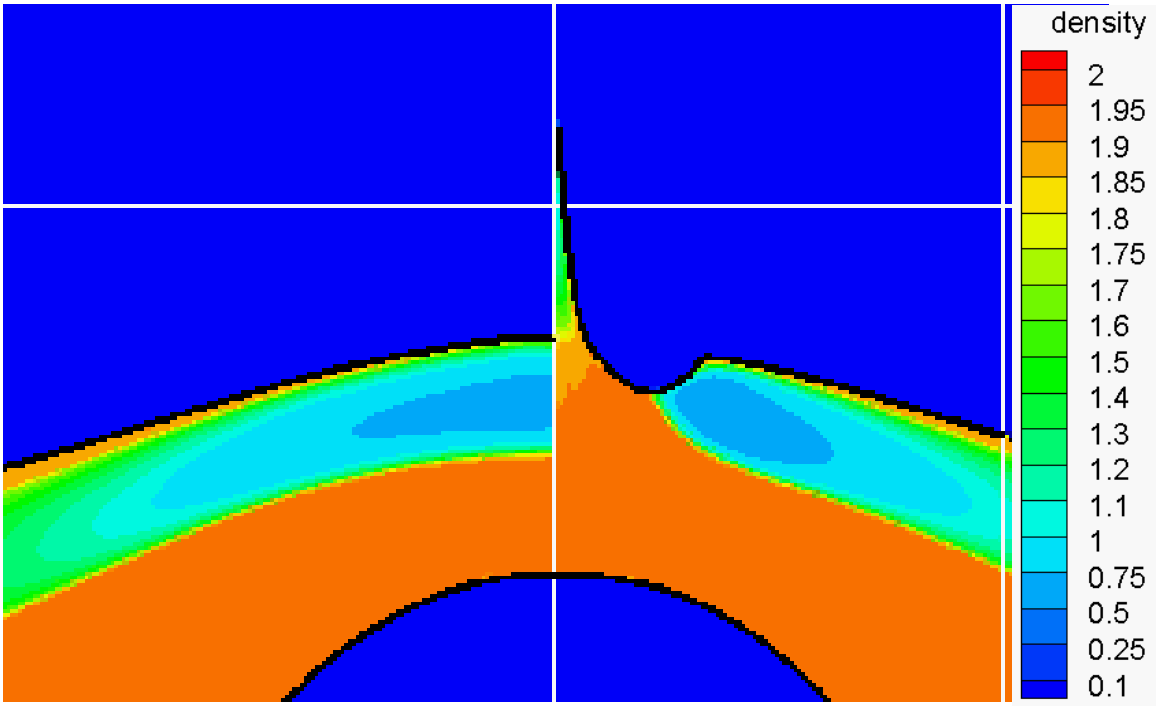

Figure 6 Detail of Dome and Jet From Lower Left View of Figure 5

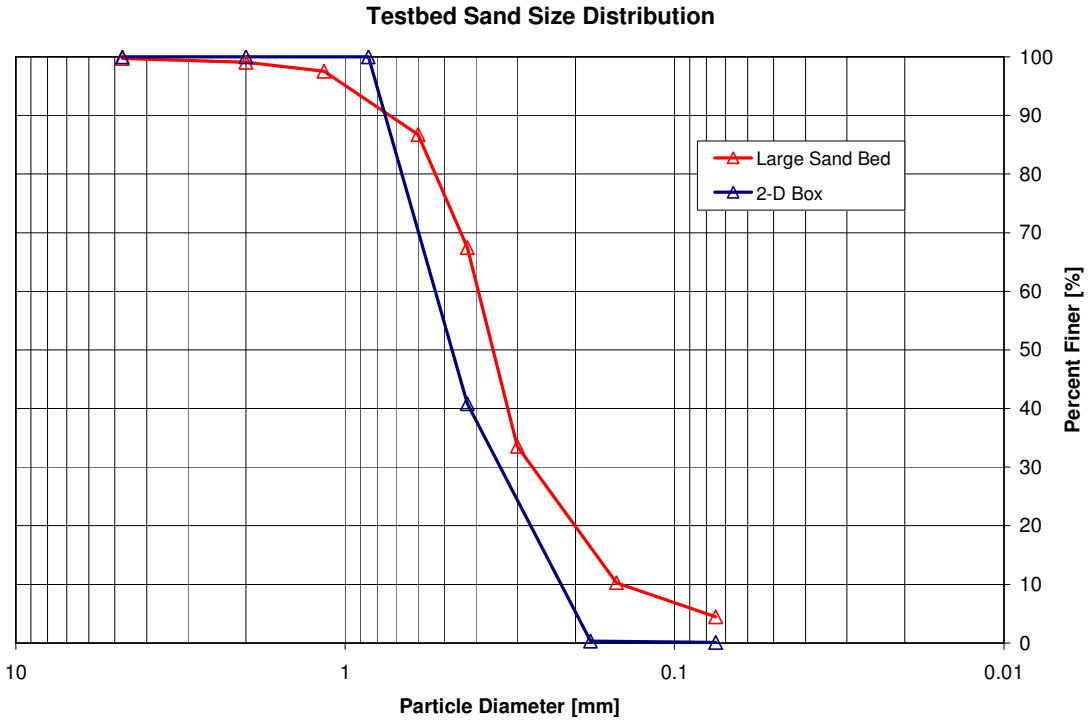

Figure 7 Sand Grain Size Distribution

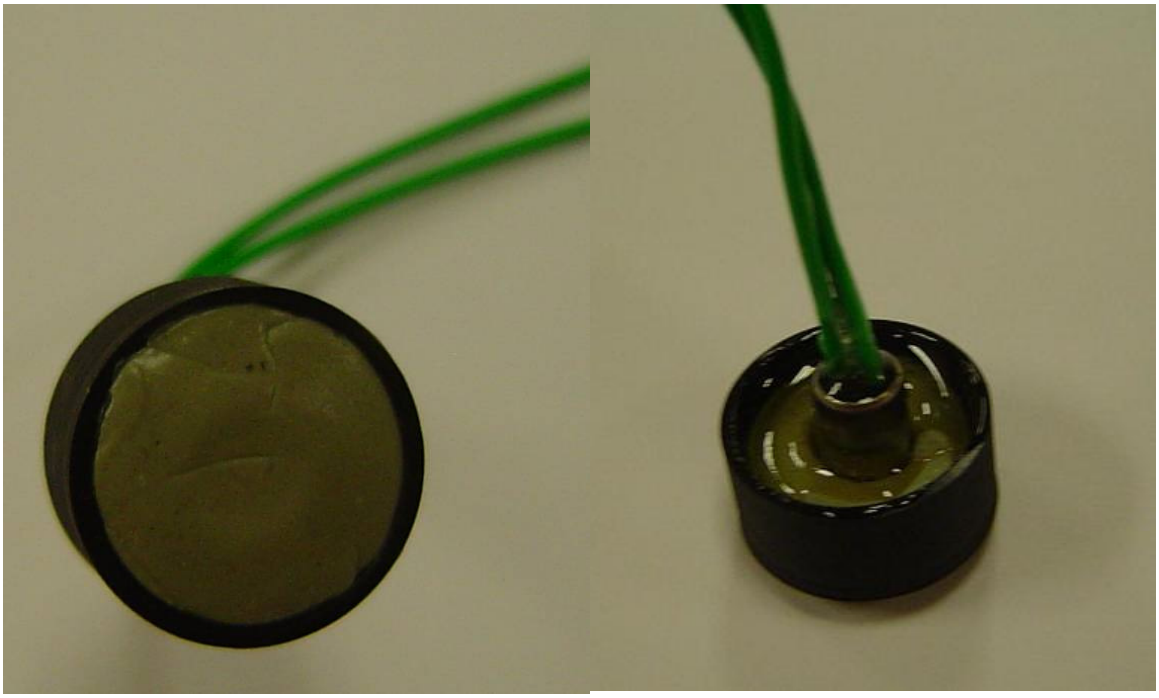

Figure 8 0.5g DETASHEET Charges

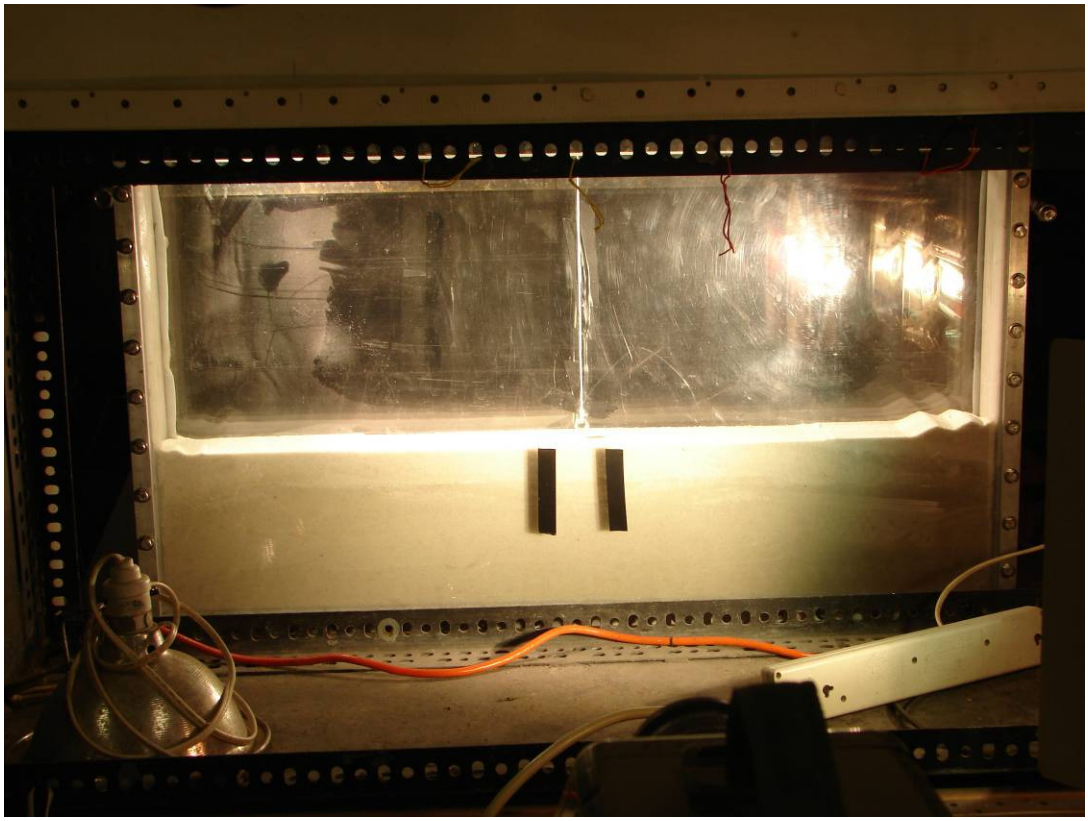

Figure 9 “2-D” Test Bed Used for Tests with 0.5g and 0.069g Charges

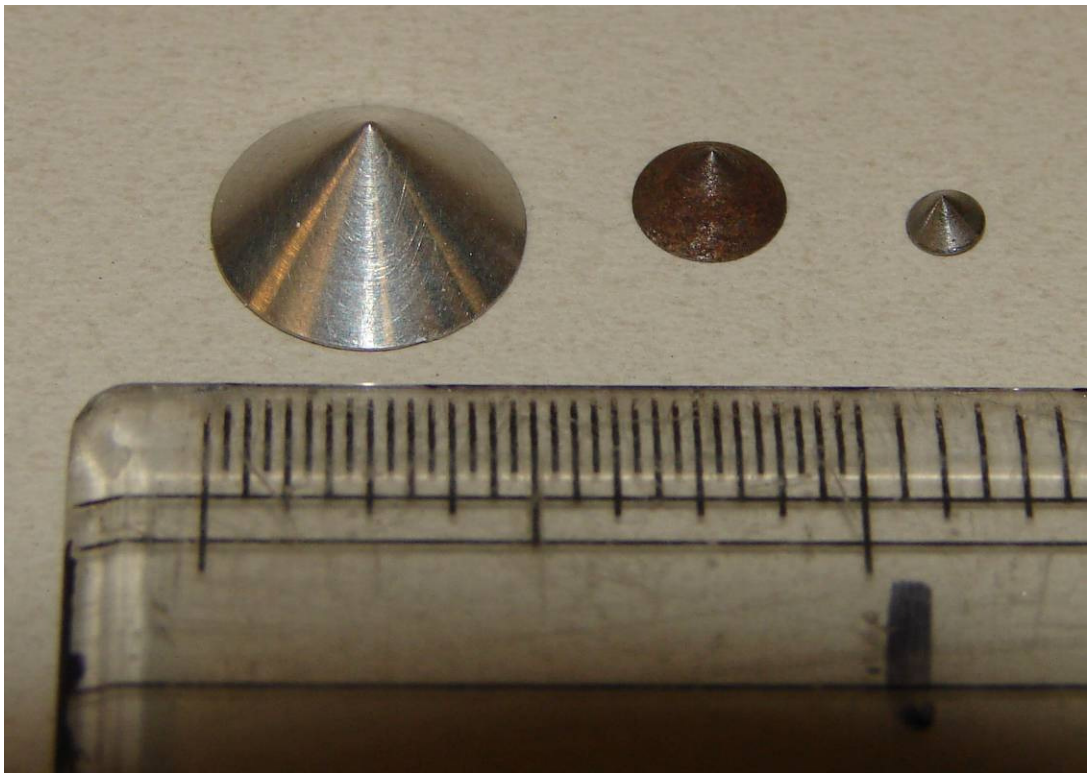

Figure 10 Forms Used to Create 0.5, 0.25 and 0.125 Depressions in Sand

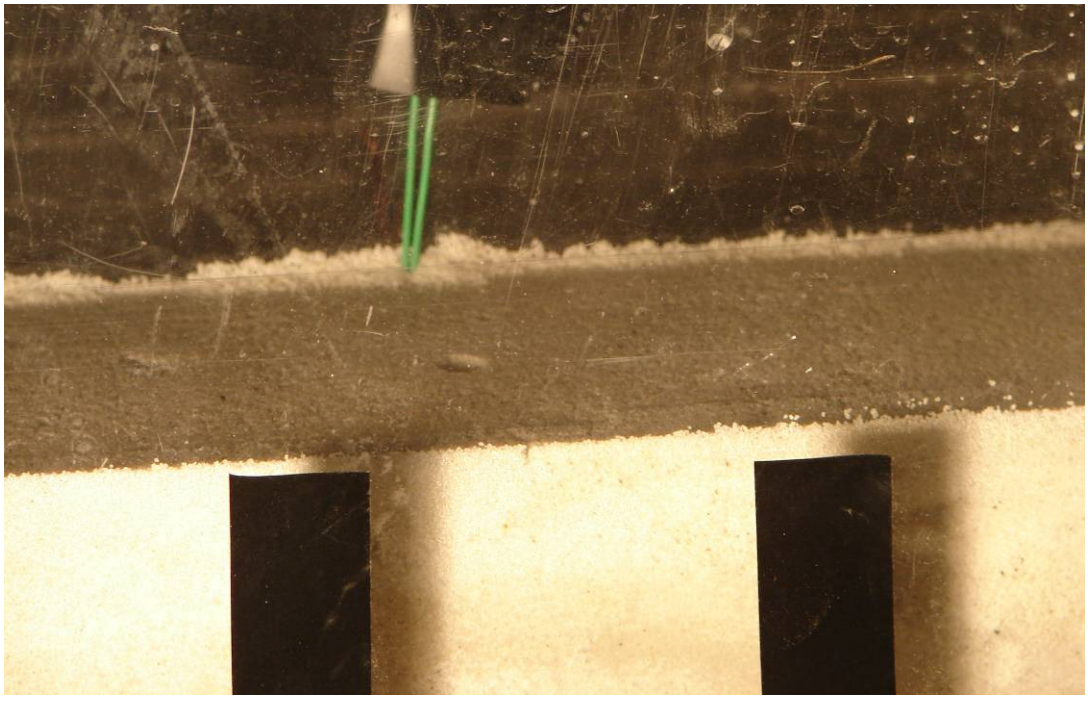

Figure 11 “2-D” Test Bed With 0.25 in. Depression in Sand Prior to Test

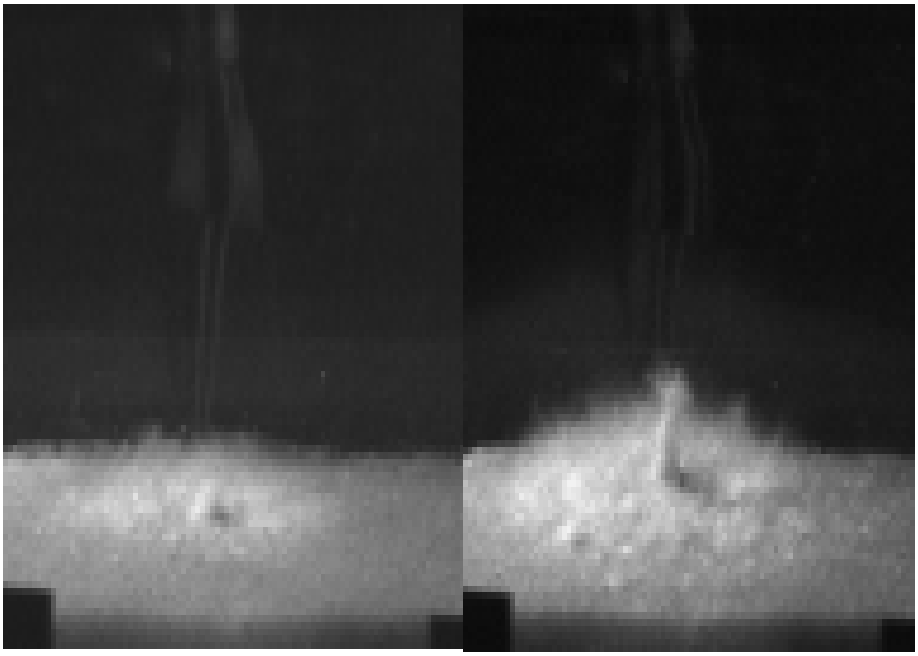

Figure 12 Jet From Dome 30 Test, 0.5g Charge, DoB = 0.5 in. at t = 73.9 and 134.8 µs After Firing

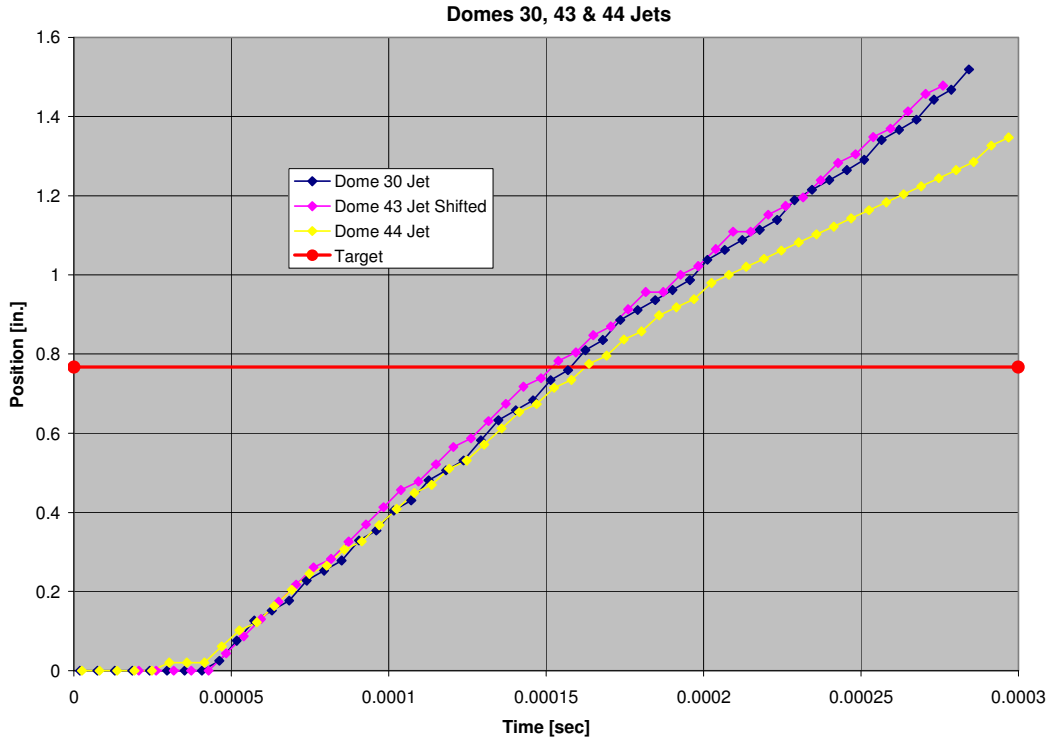

Figure 13 Position of Jet Tip vs Time, Three Nominally Identical Tests

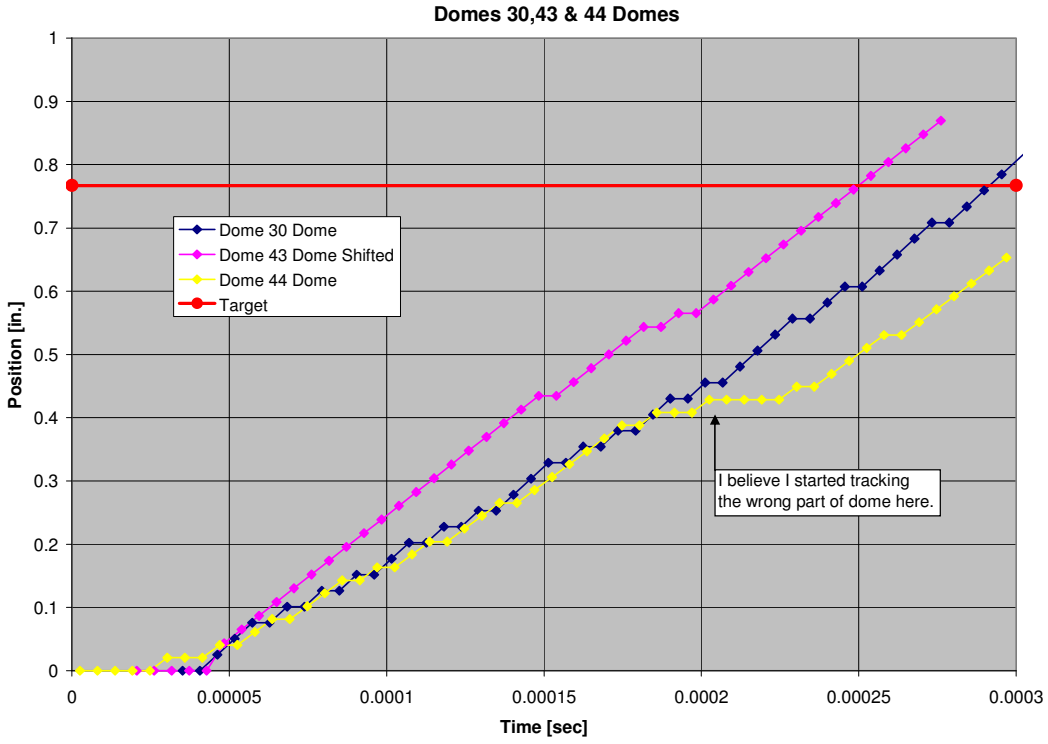

Figure 14 Position of Sand Dome, Three Nominally Identical Tests

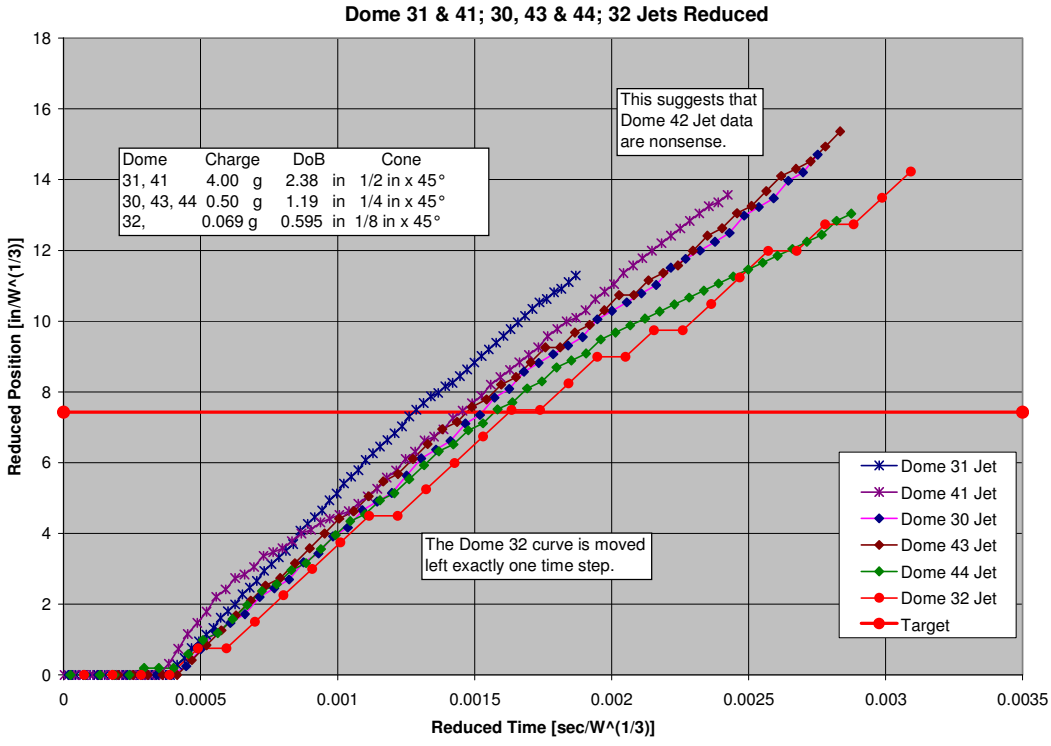

Figure 15 Reduced Positions of Jets vs Reduced Time for Scaled Tests

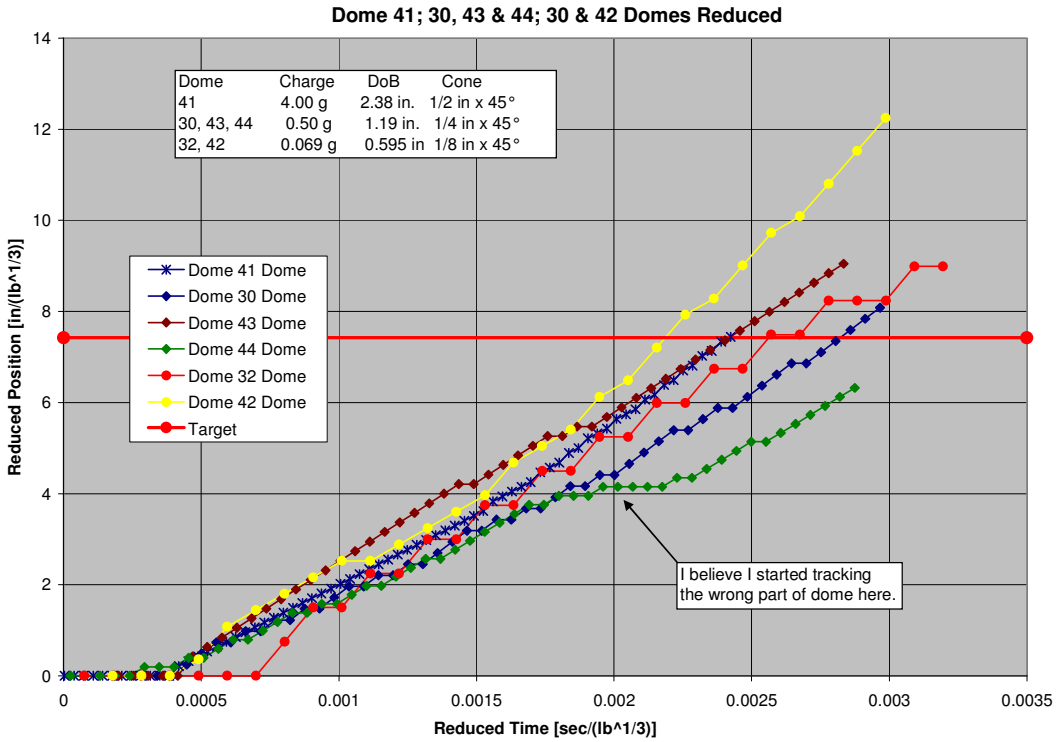

Figure16 Reduced Positions of Domes vs Reduced Time for Scaled Tests

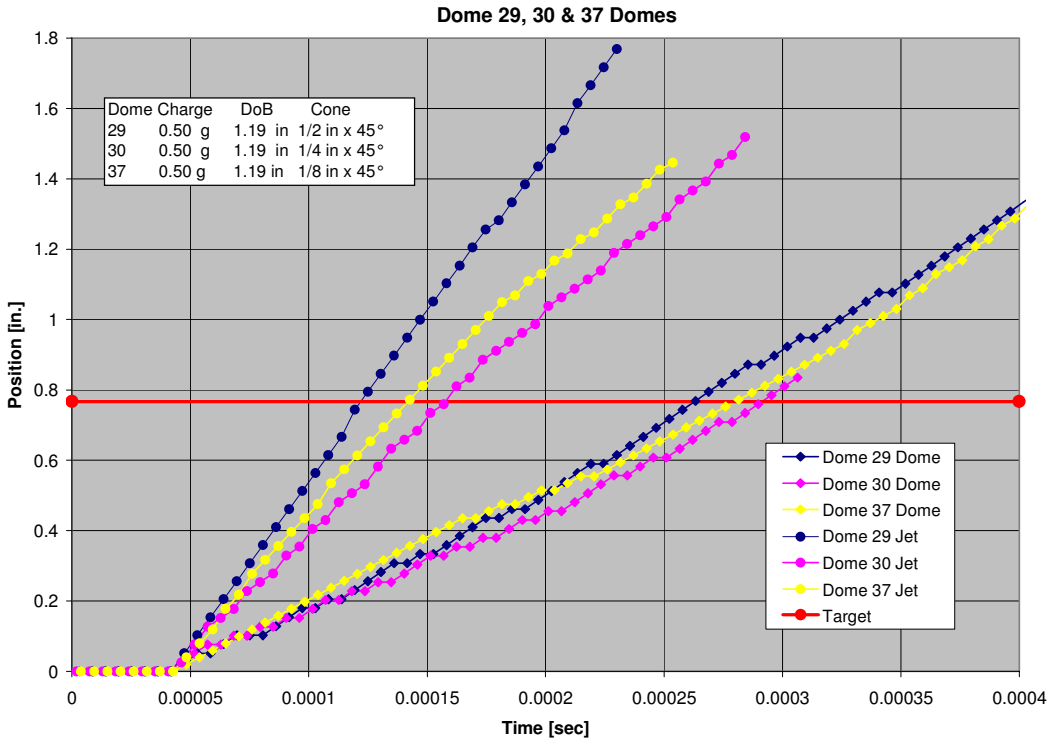

Figure 17 Position of Jets and Domes vs Time, Three Cone Sizes, All Else Same

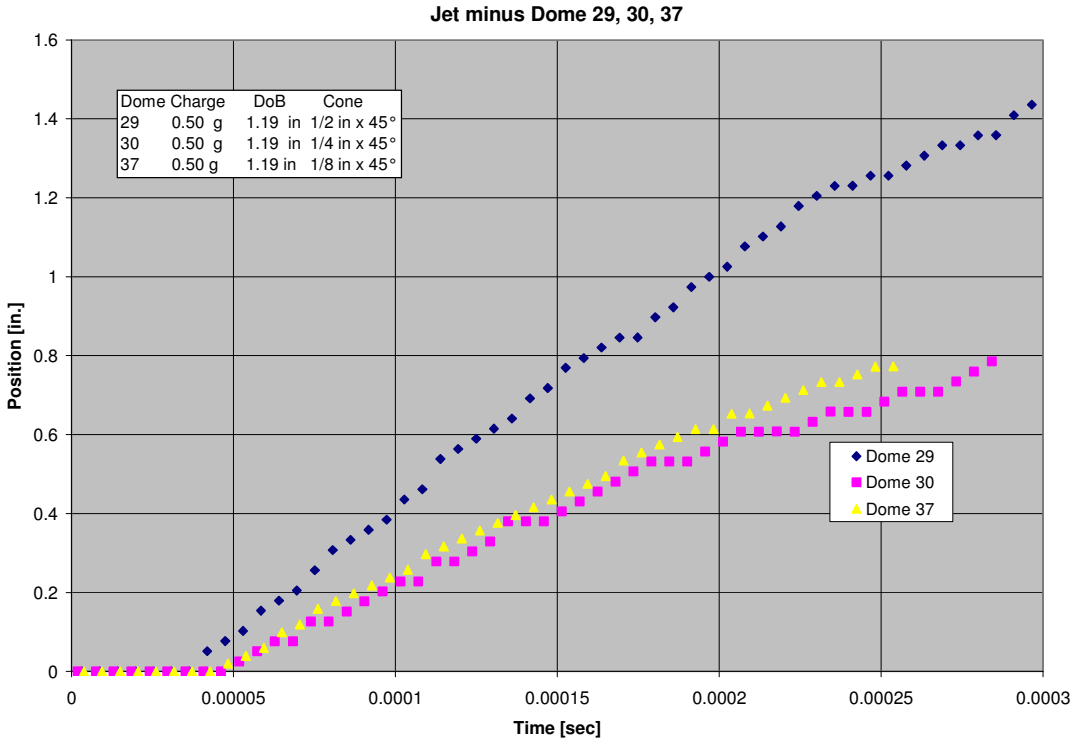

Figure 18 Position of Jets Relative to Domes, Three Cone Sizes, All Else Same

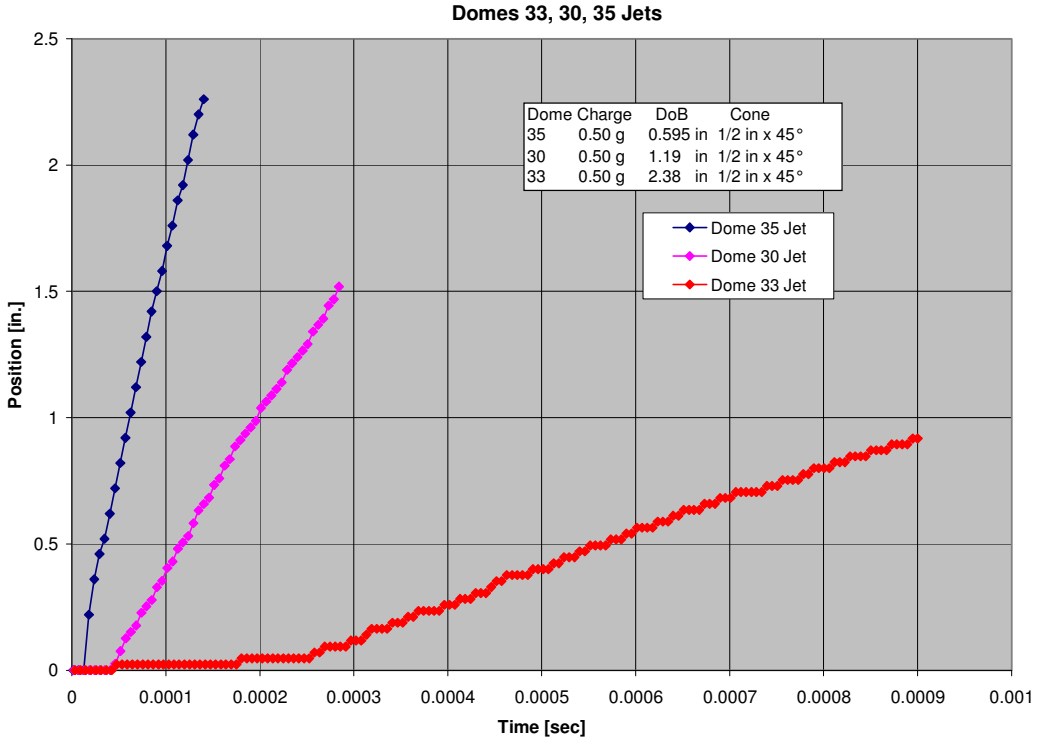

Figure 19 Position of Jets, Three Different DoBs, All Else Same

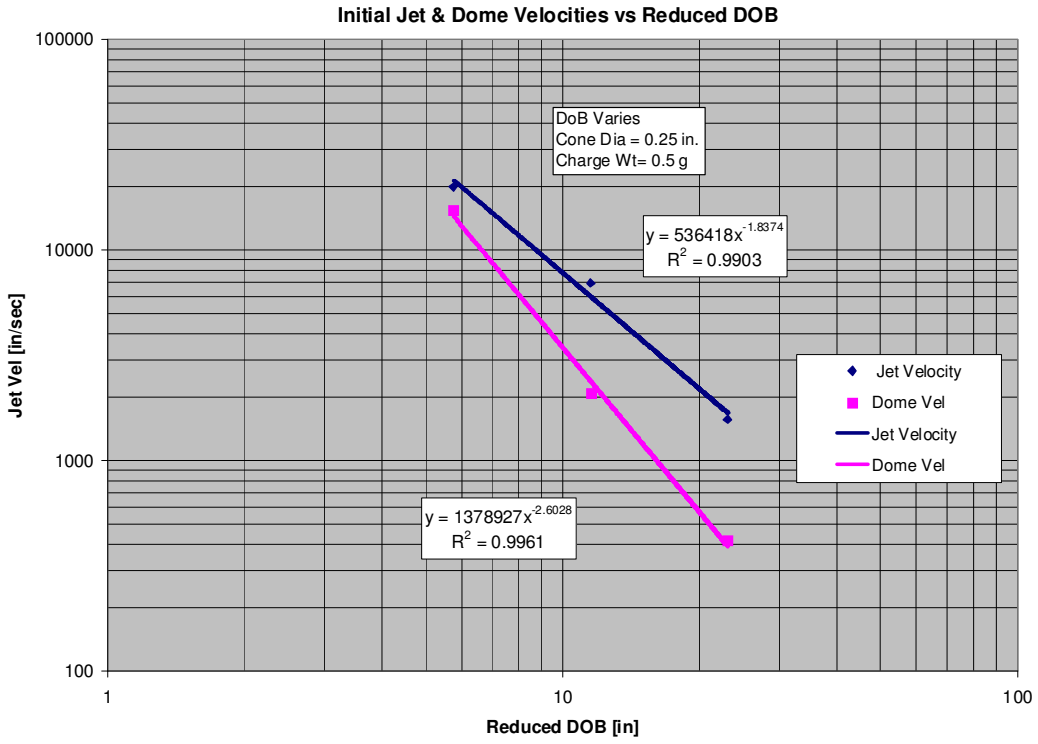

Figure20 Initial Velocity of Jets and Domes vs Reduced DoB, 0.5 in. Dia Cone and 0.5g Charge

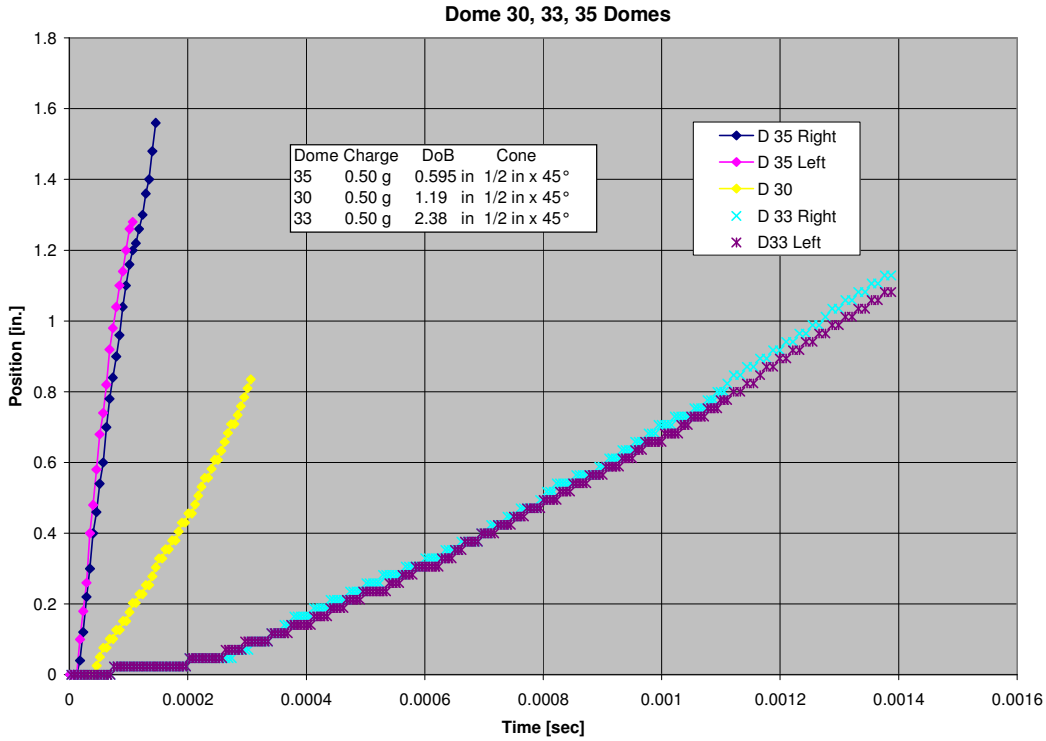

Figure 21 Position of Sand Domes Three Different DoBs, All Else Same

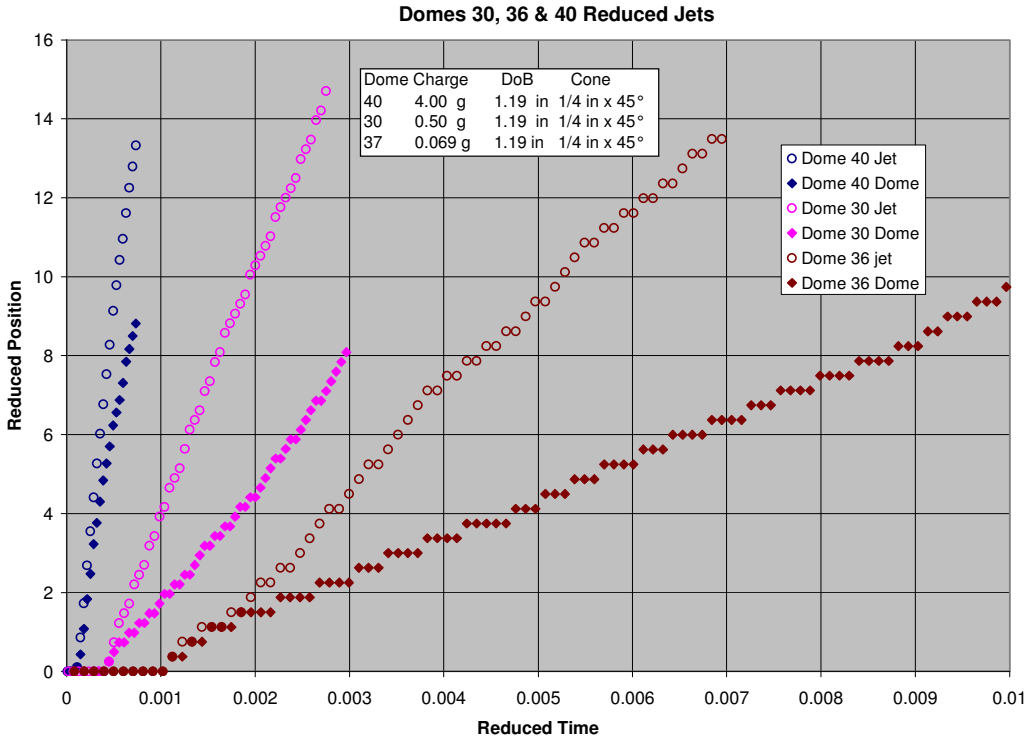

Figure 22 Position of Jets and Sand Domes, Three Different Charge Weights, All Else Same

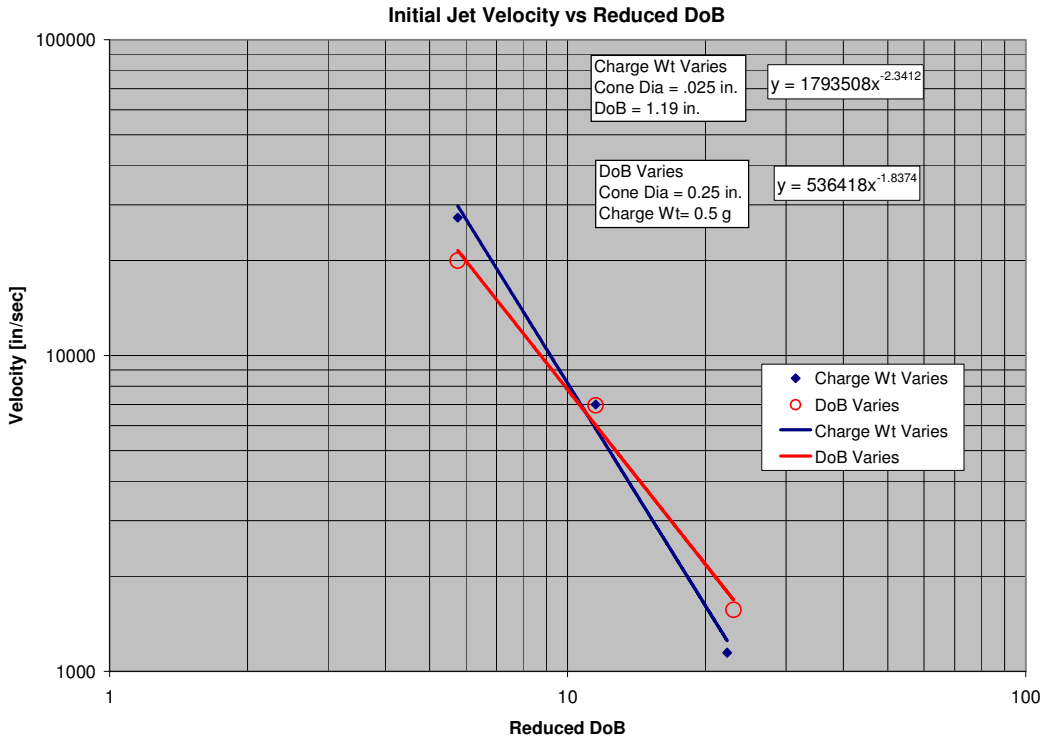

Figure 23 Initial Velocity of Jet vs Reduced DoB, Charge Weight and DoB Vary

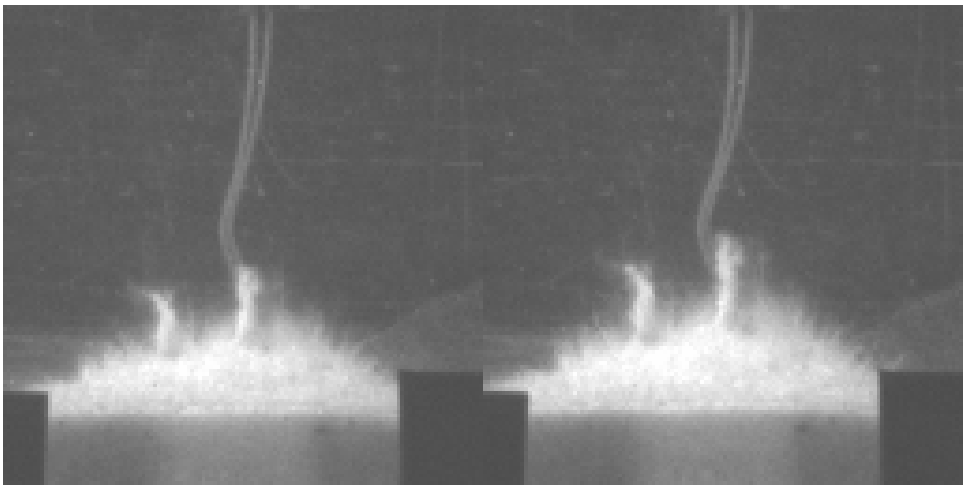

Figure 24 Test Dome 43, 0.5g DETASHEET, DoB = 1.19 in., Two Jets. t = 142.8 and 170.54 µs

Figure 25 Test Dome 44, 0.5g DETASHEET, DoB = 1.19 in., Pre-test

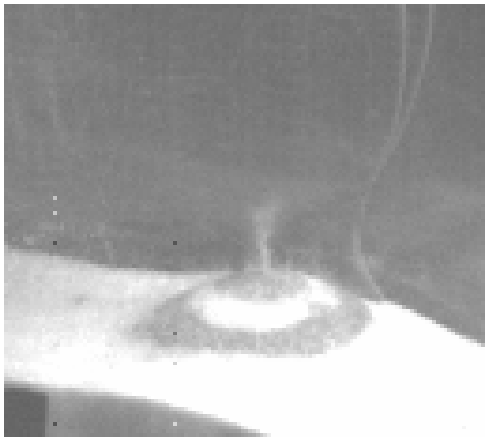

Figure 26 Test Dome 44 t = 408 µs

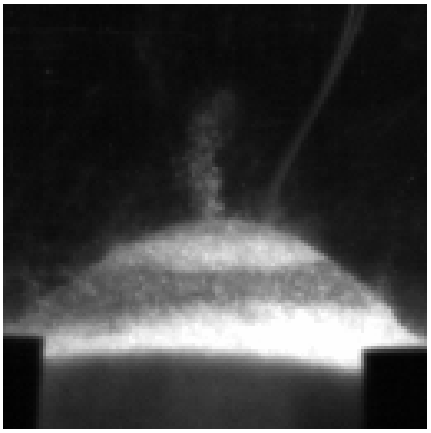

Figure 27 Test Dome 44 t = 408 µs